Journal of Alloys and Compounds 509 (2011) 5567–5570

Contents lists available at ScienceDirect

Journal of Alloys and Compounds

journal homepage: www.elsevier.com/locate/jallcom

Quickest single-step one pot mechanosynthesis and characterization of ZnTe quantum dots

S. Patra, S.K. Pradhan*

Dept of Physics, The University of Burdwan, Golapbag, Burdwan, West Bengal 713104, India

ARTICLE INFO

Article history:
Received 29 December 2010
Accepted 7 January 2011
Available online 17 February 2011

Keywords:
Nanostructured material
Mechanical alloying
X-ray diffraction
TEM
Optical properties

ABSTRACT

ZnTe quantum dots (QDs) are synthesized at room temperature in a single step by mechanical alloying the stoichiometric equimolar mixture (1:1 mol) of Zn and Te powders under Ar within 1 h of milling. Both XRD and HRTEM characterizations reveal that these QDs having size ~5 nm contain stacking faults of different kinds. A distinct blue-shift in absorption spectra with decreasing particle size of QDs confirms the quantum size confinement effect (QSCE). It is observed for first time that the QDs with considerable amount of faults can also show the QSCE. Optical band gaps of these QDs increase with increasing milling time and their band gaps can be fine-tuned easily by varying milling time of QDs.

1. Introduction

Synthesis of nanometer-sized semiconductor particles, usually known as quantum dots (QDs), and their characteristic for various applications are of great interest both for fundamental research and technical applications in electrical and optoelectronic devices because of their novel electrical and optical properties originating from quantum confinement [1–7] by which they differ significantly from their bulk properties.

ZnTe is an attractive II–VI compound semiconducting material with a direct band gap (bulk) of 2.267 eV (ca. 548 nm at room temperature) in the green region of the electromagnetic spectrum having Bohr exciton radius ~6.2 nm [8–10]. ZnTe QDs have wide range of potential applications in a variety of solid-state devices such as photodetectors, light emitting diodes [10], act as buffer layers for IR detectors and window material in a tandem solar cell [9].

Different routes like, gas-evaporation technique [11], wet chemical synthesis [8], colloidal synthesis [9], chemical vapor deposition technique [12], self assembled technique [13] had been used to synthesize ZnTe QDs. All the above preparation techniques need either heavy and costly instruments or costly chemicals and require several steps as well as long time for processing of ZnTe QDs. So, there was a constant demand on evolution of a simple and cost effective method for mass production of ZnTe QDs due to their applications in so many fields of potential interest. To the best of our knowledge, there is no report on mechanosynthesis of ZnTe QDs by mechanical alloying (MA) the elemental Zn and Te powders in a single step, in a single pot at room temperature within 1 h of milling. Thus, it is the first time report on mechanosynthesis of ZnTe QDs in a simplest as well as shortest route of synthesis. It has already been reported that different characteristics and physical properties of QDs depend on their particle size [8]. One of the advantages of the mechanosynthesis of ZnTe QDs is that one can obtain QDs with desired size explicitly by varying the milling time of QDs. In the present case, the size of ZnTe QDs obtained after 15 h of milling reduces to ~4.5 nm and HRTEM images reveal the presence of different kinds of stacking faults in these QDs. The optical characterizations of ball milled ZnTe QDs have been made with the assistance of absorption spectra of these QDs in the UV region following the method as reported earlier [14]. The blue shift in the absorption spectra depicts the confirmation of size quantization of ZnTe QDs. Optical band gap of these QDs are calculated using Tauc formula [15] applicable to direct band gap semiconductors and found to increase with increasing milling time and thus the band gap of these QDs can be fine-tuned easily by varying milling time of QDs.

The main objectives of this work are to (i) prepare the ZnTe QDs by top-down method in a record minimum time, (ii) obtain the particle sizes of QDs from XRD patterns and TEM images and (iii) investigate the blue shift in the UV–vis absorbance spectra to confirm the particle size confinement effect.

2. Experimental

Pure zinc (purity 99.5%, Loba Chem.) and tellurium powders (purity 99.5%, Sigma–Aldrich) taken in 0.5:0.5 molar ratio were used as the starting ingredients. MA is carried out at room temperature under Ar atmosphere using a planetary ball

* Corresponding author. Tel.: +91 342 2657800; fax: +91 342 2657800.
E-mail address: skp_bu@yahoo.com (S.K. Pradhan).

0925-8388/$ – see front matter © 2011 Elsevier B.V. All rights reserved.
doi:10.1016/j.jallcom.2011.01.214

mill (model-P5, M/S Fritsch, GmbH, Germany). Powders were accurately weighed under Ar and placed in a hardened chrome–steel vial of 80 ml volume kept inside the inert glove bag and mounted on the rotating disk of ball mill. Powders were milled for a pre-determined time and a part of the milled sample was taken out from the vial for X-ray measurement. The progress of milling was monitored at different interval of time, by analyzing changes in X-ray powder diffraction patterns of ball-milled samples.

The X-ray powder diffraction profiles of the unmilled mixture and ball milled samples were recorded using Ni-filtered CuK_α radiation from a highly stabilized and automated Philips X-ray generator (PW 1830) operated at 40 kV and 20 mA. The step-scan data (of step size 0.02° 2θ and counting time 5–10 s depending on the peak intensity) were recorded for the entire angular range 20° to 80° 2θ. Microstructures as well as selected area electron diffraction (SAED) patterns of the ball milled samples were carried out using high resolution transmission electron microscope (JEOL, JEM2100) operated at 200 kV, equipped with a GATAN CCD camera. For microscopy, a small amount sample was dispersed in ethanol, and then sonicated and subsequently, a drop of it was put on a carbon coated copper grid for TEM study. The absorbance spectra were recorded in a UV–vis spectrophotometer (SHIMADZU UV-1800, JAPAN) in the wavelength range 200–900 nm. Before that a small amount sample was dispersed fairly in ethanol at room temperature then kept it in the quartz cuvette of the spectrophotometer.

3. Method of X-ray analysis

In general, the experimentally observed X-ray peak broadening (β_O) (full width at half maximum (FWHM) intensity of the diffraction peak) is a convolution of (i) instrumental broadening (β_i), (ii) particle (crystallite) size broadening (β_D) and (iii) lattice strain broadening (β_S). The instrumental broadening has been estimated from the peak broadening of a specially prepared 'Si' [16] standard. The instrumental broadening correction has been made according to Warren [17] in a more precise way as:

$$\beta = \sqrt{(\beta_o^2 - \beta_i^2)}$$

where β represents the convoluted peak broadening due particle size and strain only.

The particle size and other structural parameters of ball milled samples have been calculated from respective XRD patterns using Scherrer formula and Williamson–Hall equation [18]. In Scherrer formula, the X-ray peak broadening, β (excluding β_i) is considered solely for the small particle size (D) broadening (β_D) and the contribution from lattice strain is ignored. Considering all reflections of ZnTe QDs, the average particle size is calculated using the well known relation:

$$D = \frac{k\lambda}{\beta \cos\theta} \quad (1)$$

where λ is the wave length of radiation used, k is the Scherrer constant, the peak broadening, θ is the diffraction angle of the respective peak.

The particle size as well as lattice strain has been estimated using Williamson–Hall (W–H) equation [18].

$$\beta \cos\theta = \frac{k\lambda}{\beta \cos\theta} + 4\varepsilon \sin\theta \quad (2)$$

where ε is the lattice strain. In this method, $\beta \cos\theta$ is plotted along ordinate and $4 \sin\theta$ along abscissa. The particle size and lattice strain of these QDs are obtained from the intercept of the ordinate and slope of the straight line, respectively.

4. Results and discussion

4.1. Compositional and structural studies

Fig. 1(a) shows the XRD patterns of ZnTe QDs for different durations of milling. It is clearly evident from the indexed pattern that the unmilled (0 h) powder mixture is composed of Cd (JCPDF No. 05-0674; hexagonal, Sp. Gr. $P6_3/mmc$; $a = 2.9793$ Å, $c = 5.6181$ Å) and Te (ICSD code 23058; trigonal; Sp. Gr. $P3_121$; $a = 4.411$ Å; $c = 5.934$ Å) phases. The well-resolved sharp reflections from both phases clearly indicate that particle sizes of both starting ingredients are quite large.

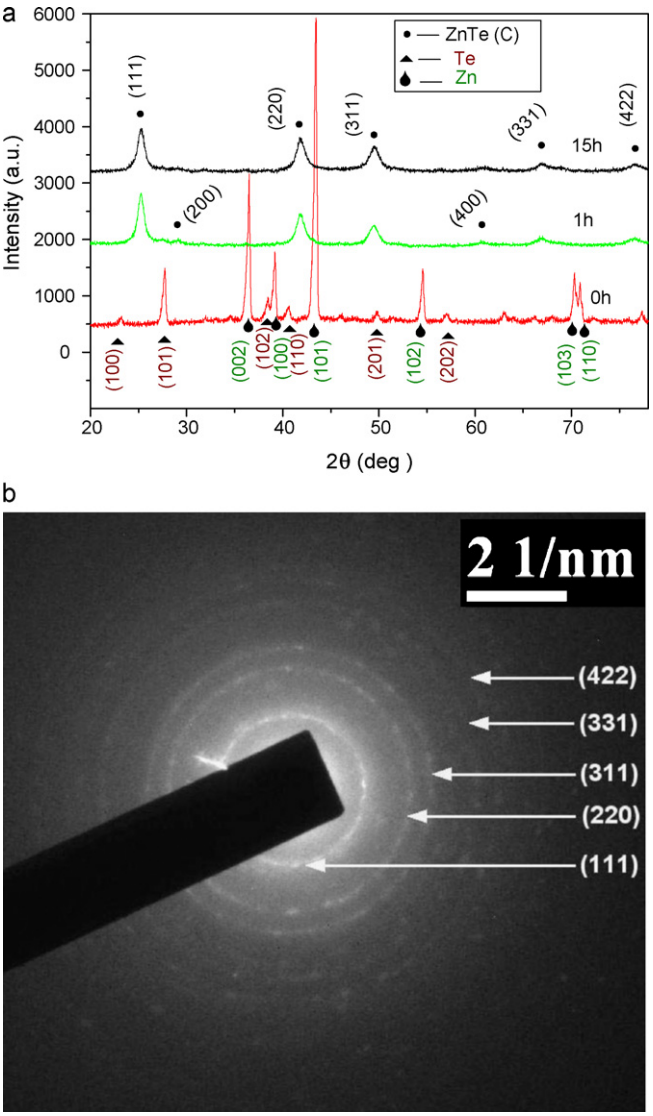

Fig. 1. a X-ray powder diffraction patterns of unmilled and ball milled Zn and Te powders (1:1 mol) milled for different durations. ZnTe (C) denotes the cubic ZnTe phase and (b) SAED pattern of ZnTe QDs obtained from 15 h milled sample.

It is very interesting to note that just after 1 h of milling the elemental powder ingredients, there is a significant change in the XRD pattern and all reflections of cubic ZnTe (ICSD code 653194, Sp. Gr. F-43m, a: 6.41 Å) phase appeared clearly with significant amount of peak broadening. As there is no reflection in the XRD pattern either from the starting ingredients or from the milling media, it confirms that the stoichiometric ZnTe phase has been formed without any contamination within a very short period of milling. It can also be noticed that in the course of milling up to 15 h, there is no significant change in XRD pattern except a small increase in peak broadening. It signifies that the ZnTe particles are initiated with a very small size and their size reduces slowly with increasing milling time.

The phase formation and contamination in ball milled samples have also been verified by the SAED pattern taken from the 15 h milled sample. The clearly indexed diffraction pattern as shown in Fig. 1(b) confirms the presence of polycrystalline cubic ZnTe phase without any contamination phase and broadened rings from individual atomic planes reveal that the size of ZnTe particles are quite small in size.

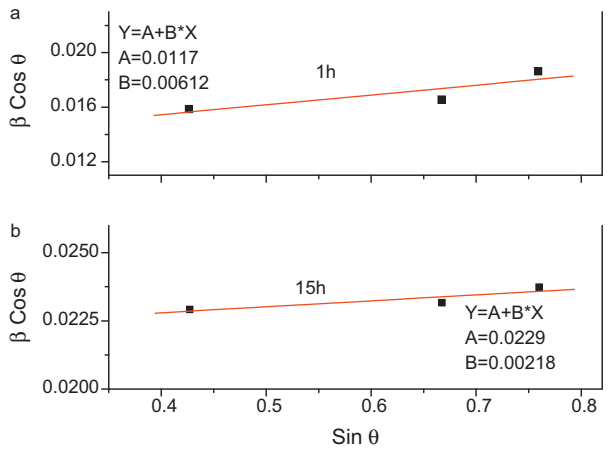

Fig. 2. The Williamson–Hall plot for (a) 1 h and (b) 15 h ball milled ZnTe sample.

Particle sizes of these QDs are estimated from the respective XRD patterns employing both Scherrer formula and Williamson–Hall equation. It is found that the particles are isotropic in nature and average particle size of milled powder obtained from Scherrer formula reduces from ~11 nm after 1 h to ~5.4 nm after 15 h of milling. From the Williamson–Hall plot (Fig. 2) it has been observed that the particle size reduces from ~11.7 nm after 1 h to ~5.9 nm after 15 h of milling. The HRTEM image (Fig. 3) of 15 h milled sample clearly reveals presence of (1 1 1) atomic planes in these almost isotropic shaped QDs. It may be noted that these QDs are very much prone to particle agglomerations, and as a result, all appeared QDs are not well resolved in the HRTEM image. However, with very careful observation, we could have identified some of the isolated particles in the images and encircled them for better expediency. An isolated particle is also shown in the inset, which is surrounded by a non-crystalline environment, like any individual ZnTe quantum dot. Sizes of these isolated QDs vary between ~4.3–5.05 nm (average size ~4.8 nm), which are very close to the average particle size obtained from X-ray analysis. In both the cases, the obtained particle size is less than that of the Bohr exciton radius of ZnTe (~6.2 nm).

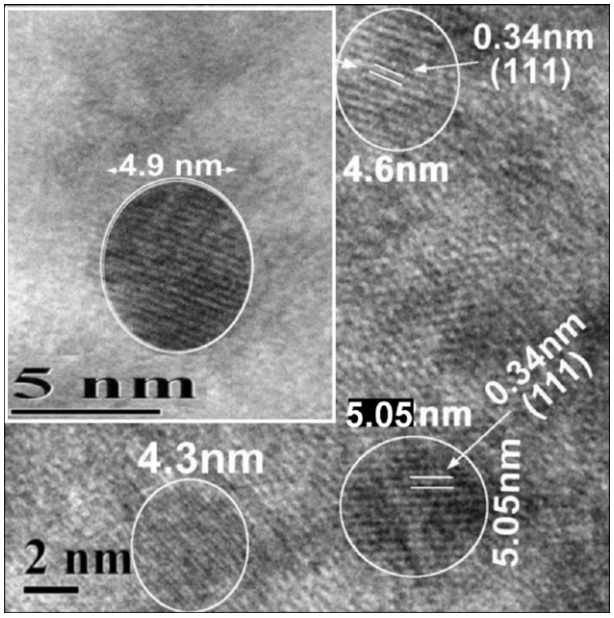

Fig. 3. TEM image taken from a selected zone depicts the presence of almost spherical particles (shown in circular mark) in 15 h ball milled sample. A single QD has been shown in inset.

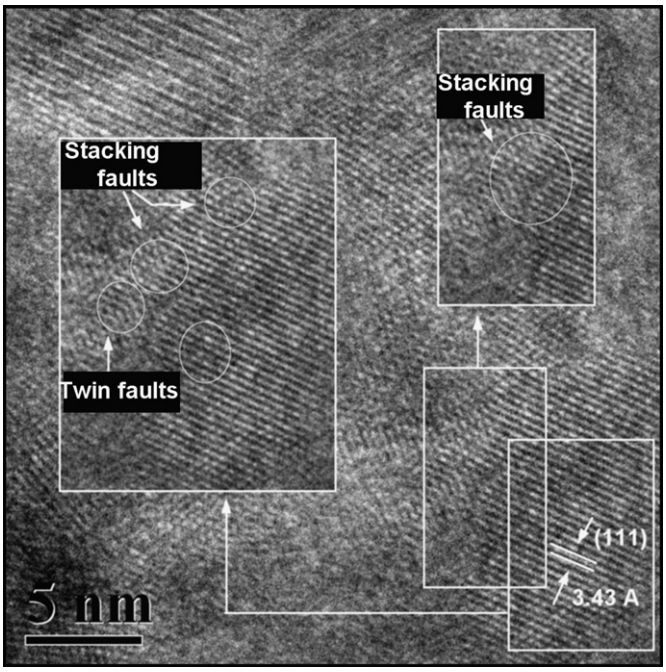

Fig. 4. Highly stacking fault and twin faults region in (1 1 1) plane of cubic Znte QDs.

It is also obvious that the distribution of particle size is quite narrow in HRTEM image (Fig. 3). Thus, almost mono-dispersed ZnTe isotropic particles with ~5 nm size can be obtained by this top-down physical method, like any chemical route of preparation [8–14]. In our earlier studies [19–21], we have reported the formation of mono-dispersed ZnS, CdS and CdTe QDs by this method of preparation.

The lattice strain in ZnTe QDs obtained from W–H plot (Fig. 2) is $\sim 1.53 \times 10^{-3}$ for 1 h milled sample and that for 15 h is $\sim 0.545 \times 10^{-3}$. This kind of decrease in lattice strain with increasing milling time has also been observed in case of ZnS [19] QDs and may be attributed to release of lattice strain due to agglomeration of QDs at higher milling time. It signifies that the as prepared ZnTe QDs are almost free from lattice strain.

It has been reported earlier that due to high degree of impact of milling process the mechano-synthesized QDs contain different kinds of stacking faults [19–21]. In the present study, presence of different kinds of stacking faults in the 15 h ball milled ZnTe QDs is also revealed clearly in different areas of the HRTEM image (Fig. 4). The presence of several grain boundaries in Fig. 4 depicts that the material is polycrystalline in nature. Both stacking faults and twin faults are generated on (1 1 1) plane of cubic ZnTe in the course of milling. It indicates that the as prepared QDs contain lattice imperfections of different kinds which can influence the property of QDs to a great extent.

4.2. Size confinement and optical band gap studies

The optical absorption spectra of the ZnTe nanoparticles are recorded as a function of wavelength in the wavelength range (200–900 nm) as shown in Fig. 5. The absorption is expected to depend on different factors, such as, surface roughness and dispersion effect. The lower value of absorption in case of ZnTe nanoparticles could be due to light scattering on the rough surface. The absorption peak for 1 h milled sample (particle size ~11 nm) appears at 367.5 nm and that for 15 h (particle size ~5.4 nm) milled sample at 351.5 nm. It indicates that the absorption edges are shifting towards shorter wavelength region, i.e. a significant blue-shift is clearly observed with decreasing size of ZnTe particles.

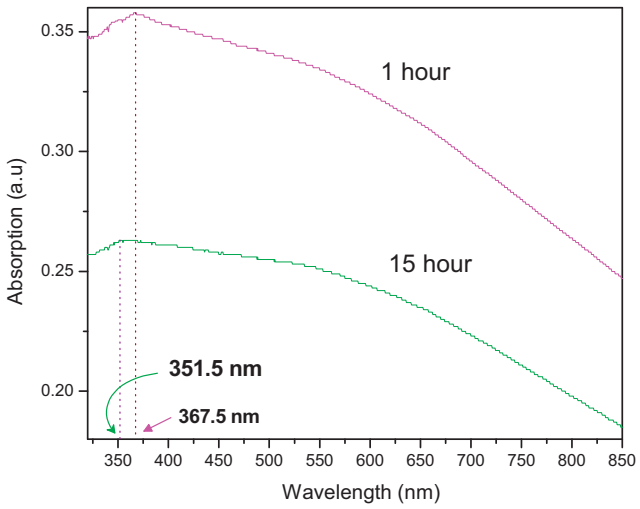

Fig. 5. UV–vis absorption spectra of ZnTe QDs ball milled for 15 h and dispersed in ethanol.

It is also seen in Fig. 5, the onset of effective transition edge indeed shifts from greenish (~548 nm corresponds to 2.265 eV) for bulk ZnTe [8–10] to UV region for the ball milled ZnTe QDs. Both the observed blue shift of absorption edge and the absorption peaks can be attributed to the quantum confinement effect (QCE). Again, the appearance of the UV–vis absorption peak is a sign of monodispersity [22] which also agrees well with the TEM and XRD studies.

The average optical band-gaps of these QDs are obtained from the absorption peak position of UV–vis spectroscopy using the Tauc [15] formula, applicable to direct band-gap semiconductors. The calculated band gaps are 3.37 eV and 3.52 eV for 1 h and 15 h ball milled samples, respectively. This result indicates that the band gaps of the ZnTe QDs exhibit a marked blue shift with respect to that of the bulk and this blue shift could be attributed to QSCE, which is most essential feature of the QDs.

5. Conclusions

The cubic ZnTe QDs are synthesized for the first time by mechanical alloying the elemental Zn and Te powders in a single pot of ball mill at room temperature in a single step within 1 h of milling. Both XRD analysis and HRTEM images reveal that shape of ZnTe QDs is isotropic in nature and particle sizes of these QDs reduce to ~5 nm with a very narrow size distribution after 15 h of milling. The existence of stacking faults and twin faults are obvious from HRTEM image which is being reported for the first time that the QDs with considerable amount of faults can also show the QSCE. As the sizes of these QDs are quite below the calculated Bohr exciton radius of ZnTe, these QDs show quantum confinement effect and optical band gap of these QDs are very different from their bulk counterpart. It is thus possible to have tunability on the opto-electronic properties of ZnTe QDs only by varying the particle size of QDs which is synchronous with the duration of milling.

Acknowledgements

Authors wish to thank the University Grants Commission (UGC) India, for providing research fellowship and granting DSA-III programme under the thrust area “Condensed Matter Physics including Laser applications” to the Department of Physics, Burdwan University under the financial assistance of which the work has been carried out. Authors also acknowledge CRF, IIT Kharagpur, India for providing HRTEM facility.

References

[1] L.E. Brus, Appl. Phys. A 53 (1991) 465–474.
[2] A.P. Alivisatos, J. Phys. Chem. 100 (1996) 13226–13239.
[3] H. Weller, Adv. Mater. (Weinheim, Ger.) 5 (1993) 88–95.
[4] A.K. Ekimov, A.L. Effros, A.A. Onuschenko, Solid State Commun. 56 (1985) 921–924.
[5] X. Peng, L. Manna, W.D. Yang, J. Wickham, E. Scher, A. Kadavanich, A.P. Alivisatos, Nature 404 (2000) 59–61.
[6] L. Manna, E.C. Scher, A.P. Alivisatos, J. Am. Chem. Soc. 122 (2000) 12700–12706.
[7] L. Brus, IEEE J. Quantum Electron. QE-229 (1986) 1909–1912.
[8] J. Zhang, K. Sun, A. Kumbhar, J. Fang, J. Phys. Chem. C 112 (2008) 5454–5458.
[9] Y.W. Jun, C.S. Choi, J. Cheon, Chem. Commun. 101 (2001).
[10] T. Mahalingam, V.S. John, S. Rajendran, P.J. Sebastian, Semicond. Sci. Technol. 17 (2002) 465–471.
[11] S. Hayashi, H. Sanda, M. Agata, K. Yamamoto, Phys. Rev. B 40 (1989) 5544–5548.
[12] M.C. Harris Liao, Y.H. Change, C.C. Tsai, M.H. Chieng, Y.F. Chen, J. Appl. Phys. 86 (1999) 4694–4696.
[13] T.W. Kim, D.C. Choo, D.U. Lee, H.S. Lee, M.S. Jang, H.L. Park, Appl. Phys. Lett. 81 (2002) 487–489.
[14] L. Li, Y. Yang, X. Huang, G. Li, L. Zhang, J. Phys. Chem. B 109 (2005) 12394–12398.
[15] P. Singh, A. Kumar, A. Kaushal, D. Kaur, A. Pandey, R.N. Goyal, Bull. Mater. Sci. 31 (2008) 573–577.
[16] J.G.M. Van Berkum, Strain fields in crystalline of materials, Ph.D. Thesis, Delft University of Technology, The Netherlands, 1994.
[17] B.E. Warren, X-ray Diffraction, Wesley, Reading, MA, 1969.
[18] A.R. Balu, V.S. Nagarethinam, A. Thayumana, K.R. Murali, C. Sanjeeviraja, M. Jaychandran, J. Alloys Compd. 502 (2010) 434–438.
[19] S. Patra, B. Satpati, S.K. Pradhan, J. Appl. Phys. 106 (2009) 034313–034318.
[20] S. Patra, B. Satpati, S.K. Pradhan, J. Nanosc. Nanotechnol. 11 (2011) 1–10.
[21] S. Patra, S.K. Pradhan, J. Appl. Phys. 108 (2010) 083515–083523.
[22] Z. Deng, Y. Zhang, J. Yue, F. Tang, Q. Wei, J. Phys. Chem. B 111 (2007) 12024–12031.